JOURNAL OF PROPULSION AND POWER
Vol. 24, No. 4, July–August 2008

Increasing Gas Turbine Blade Damping Through Cavities Filled with Viscoelastic Materials

A. Nashif*
Universal Technology Corporation, Cincinnati, Ohio 45402
P. Torvik†
Universal Technology Corporation, Xenia, Ohio 45385
U. Desai‡
PPG Industries, Inc., Allison Park, Pennsylvania 15101
and
J. Hansel§ and J. Henderson¶
Universal Technology Corporation, Dayton, Ohio 45432

DOI: 10.2514/1.35285

To evaluate the effectiveness of high-damping materials as candidate fill materials for hollow fan blades, test specimens in the form of flat trapezoidal plates were designed and mounted as cantilevers. An open-ended cavity of uniform thickness comprised 71% of the planform area. Two viscoelastic materials were developed and used as fillers. Each was modified for reduced density and then aged after application to simulate the influence of 4000 service hours at a characteristic mission profile. Values of the loss factor (reciprocal of the system quality factor) determined from the resonant responses of the filled plates in the first bending, first torsion, and second bending modes at 75°C (170°F) were found to be in the range of $\eta = 0.025$–0.045 ($Q = 22$–40), $\eta = 0.06$ ($Q = 16$), and $\eta = 0.09$–0.11 ($Q = 9$–11) for the three modes, respectively, which is an improvement of 1.5 to 2 orders of magnitude over values measured with the unfilled specimens. A finite element analysis, using temperature and frequency dependent properties of the filler material as determined by separate tests, showed satisfactory agreement with the observed values for temperatures up to 120°C (250°F). This study confirmed that the addition of viscoelastic filler to a hollow plate can increase damping significantly and that the system response could be predicted by finite element analysis. Through appropriate selection of the filler material, such systems can be designed to have maximum damping at a desired specific combination of temperature and frequency.

Nomenclature

D_D	=	energy dissipated per cycle in the fill material
D_{unf}	=	energy dissipated per cycle in the unfilled blade
E	=	real part of complex Young's modulus of filler material
g	=	gravitational acceleration
Q	=	system quality factor (inverse of loss factor)
U_D	=	peak energy stored in the dissipative fill material
U_T	=	total peak energy stored in the plate and filler
U_{unf}	=	peak energy stored in the unfilled hollow plate
η	=	loss factor
η_{mat}	=	loss factor of the filler material, measured by separate test
η_{sys}	=	loss factor of the entire system, predicted or observed
η_{unf}	=	loss factor of the unfilled plate, observed

Presented as Paper 5037 at the 43rd AIAA/ASME/SAE/ASEE Joint Propulsion Conference & Exhibit,, Cincinnati, OH, 8–11 July 2007; received 24 October 2007; revision received 18 January 2008; accepted for publication 21 January 2008.

*Consultant, 9698 Ash Court.
†Consultant, 1866 Winchester Road. Fellow AIAA.
‡Group Leader, Engineered Materials Solutions, 4325 Rosanna Drive.
§Test Engineer, 1270 Fairfield Road.
¶Senior Program Manager, 1270 Fairfield Road. Member AIAA

I. Introduction

IT HAS been proposed [1] that blades used in gas turbine engines might be constructed with a thin cavity to be filled with a high-damping material. Although not included in a rotating component, the concept has been applied. A hollow fan outlet guide vane with a vibration-damping composite material (epoxy-amine composite filled with special cavity fillers) was proposed for Airbus A380 engines. The room-temperature damping of a rectangular plate with cavities filled with a viscoelastic material (VEM) has been considered [2], both analytically and by experiment. System quality factors (Q) as low as 25–50 have been predicted and observed [3] for a hollow fan blade with a cavity filled with a viscoelastic material, as shown in Fig. 1. Several aspects of this methodology merit further study; some are considered in this investigation.

The first objective of this work was to design and fabricate relatively simple bladelike specimens that could be filled with a lightweight material having significant capacity to dissipate vibratory energy and to measure the impact of various filler materials on the response of the simulated blades to vibratory excitation. Such comparisons would assist in the selection of the best fill material for a given application. The second objective was to determine if such filler materials would retain high levels of damping after exposure to a time–temperature profile characteristic of typical aircraft missions. Achievement of this objective would suggest that such fill materials should perform successfully in an actual blade. The third objective was to ascertain if the enhanced damping of a simple bladelike specimen could be adequately predicted by finite element analysis using values of filler material properties obtained by standard testing methods. Achievement of this objective would provide encouragement that the response under service conditions of an actual blade with filler could be predicted a priori.

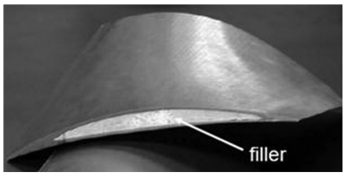

Fig. 1 Concept: hollow blade with high damping filler (after Rongong and Williams [3]).

II. Development of Test Specimens and Materials

A. Hollow Specimen Design, Fabrication, and Screening

One objective of this study was the development of test specimens that could be used to compare the effectiveness of candidate filler materials. Ideally, the test specimen should allow a consistent, uniform fill with candidate materials, yet have mode shapes and frequencies somewhat characteristic of those of actual blades. The design chosen was an open-ended hollow plate with a span of 244 mm (9.6 in.), a thickness of 11.4 mm (0.45 in), and an aspect ratio of about 2:1, with a 51 mm (2 in.) section to be clamped when mounted for testing as a cantilever plate. The cavity is of uniform thickness, is 56% of the total plate thickness, and occupies 71% of the cantilevered area. The critical planform dimensions are given in Fig. 2.

The specimens were assembled from two pieces of 6061 aluminum, one being a mirror image of the other, such that when welded along the two long edges a (partially) hollow plate is formed, as shown in Fig. 3. Six specimens were constructed.

The mode shapes and natural frequencies for the unfilled plates were predicted by finite element analysis. The first three modes were found to be, respectively, first bending, first torsion, and second bending. The deformations in next two modes were found to be primarily panel deformations of the face sheets, with chordwise bending deformations in these two modes out of phase, and in phase, respectively. Some differences from the mode shapes of a rectangular plate were evident, increasing, as expected, with mode number.

As the specimens were to be used for comparing the effectiveness of candidate fill materials, it was essential that there be no significant differences between the hollow plates before filling. Screening tests were conducted by clamping the first 2 in. of the section into a fixture mounted on a large shaker. Natural frequencies and loss factors were determined for all of the plates in each of the first several modes from the frequency response functions resulting from excitation at a low level of constant base acceleration (0.05 g). A more complete description of test equipment and procedures is given in Sec. III.

Because of inconsistencies in fabrication, principally in the welding, variations were found among the natural frequencies and loss factors of the six unfilled plates. At room temperature, the natural frequencies showed a variation (maximum to minimum) of about 7.5% for mode 1 (first bending), about 5% for mode 3 (second bending), and about 7% for mode 4. The system loss factors for the first six modes of each plate were also determined and found to be as shown in Fig. 4a.

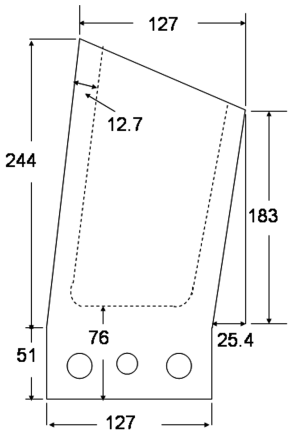

Fig. 2 Test specimen planform (mm).

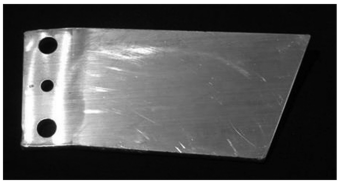

a) Plan view

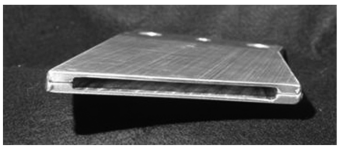

b) End view

Fig. 3 Test specimen before filling.

All of the tests were repeated to establish consistency. The numbers in parentheses in the legends of Fig. 4 indicate the total number of independent measurements. Examination of the data showed that the large variations in the loss factor (LF) were primarily due to two plates with abnormally low frequencies and high damping and a third plate with a higher frequency and lower damping. The three plates of intermediate stiffness were selected for further testing. The loss factors for the retained plates (2, 5, and 6) were found to be as shown in Fig. 4b, with the number of individual measurements shown in parentheses. The average loss factor of plate 6 (0.004) was somewhat higher than that of plate 5 (0.0037) and plate 2 (0.003). Plates 2 and 6 were chosen for use with the filler materials. Plate 5 was retested at an elevated temperature to verify that the loss factor of the unfilled plate was not influenced by thermal expansions in the clamping configuration.

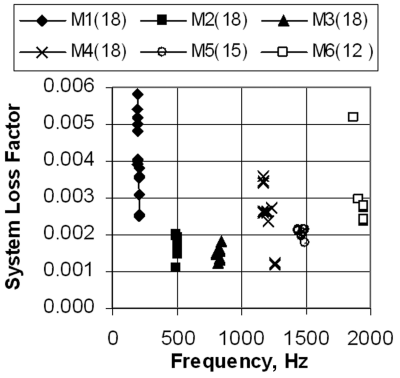

a) All plates, as fabricated

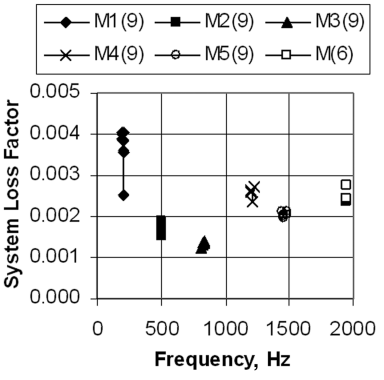

b) Selected plates only

Fig. 4 Loss factors of unfilled plates (all modes at room temperature).

B. Selection and Refinement of Filler Materials

Because all of the edges of an actual blade, and the two edges approximately perpendicular to the fixed end of the test specimen, are enclosed, the state of strain in the fill material is not that of the core of a sandwich beam, for which shear strains provide the dominant damping mechanism. Rather, it is assumed that the filler material inside a hollow fan blade is likely to be deformed primarily by normal strains, as in a free-layer treatment. Accordingly, the critical material property for high system damping in both cases can be expected to be a high value of material loss modulus. As it is also desirable to reduce blade weight, a suitable fill material must also retain good damping properties when modified so as to reduce density. For ease in filling, the material must be obtainable in liquid form. Further, to obtain well-filled blades, the material should have little or no solvent. And finally, the material must have the ability to resist mission profile times at operational temperatures.

The identification of suitable materials to be used as the viscoelastic cavity fill began with the selection of a specific mission profile and, from that, a time history of peak blade temperatures. The combination selected led to the distribution of peak service temperatures up to 149°C (300°F), shown in Fig. 5, for a service life of 4000 h.

Consideration of the five critical attributes given led to the identification of six candidate materials of two types: waterborne materials with little solvent and epoxy-based materials without solvents. The material properties of each were determined using the Öberst beam, or symmetric free-layer, technique [4]. Coatings of 0.25 mm (10 mil) or less were applied to both sides of flat strip steel specimens, nominally 200 by 13 by 0.76 mm (8 by 0.5 by 0.03 in). The specimens were then mounted as cantilever beams and excited in the second through fifth resonances (<2000 Hz) at selected temperatures in the range of −18–149 °C (0–300°F). At each temperature, the available modes of beam vibration were excited and the modal damping and frequency values measured. From these and the beam geometry, material properties of the coating materials (storage modulus, loss factor, and loss modulus) were determined from the Öberst equations at each combination of frequency and temperature. A reduced frequency nomogram for each of the 12 materials was then developed from the raw test data by using the temperature–frequency shift factor [5].

As the most relevant single parameter for this application is the loss modulus (i.e., the product of the loss factor and storage modulus), the final selection of candidate materials was made on this basis. Comparisons were made at 1000 Hz, a frequency characteristic of the third mode for the filled specimens. Values of the loss modulus at 1000 Hz over the temperature range of interest as extracted from the nomograms for each of the 12 materials are shown in Fig. 6. Material product designators are those of PPG Industries, Inc. (PPG). One material from each class was found to have a more uniform and generally higher loss modulus over the temperature range of interest, with particular emphasis on the higher temperatures. Consequently, material 05-271-65B from the epoxy-based series and material 06-64-40A from the waterborne series were chosen for further development. These materials are identified in Fig. 6 by the wide lines. The properties of the rejected materials are identified by thin lines.

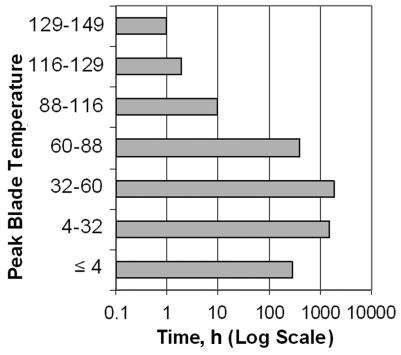

Fig. 5 Estimated times at various temperatures for 4000 service hours (°C).

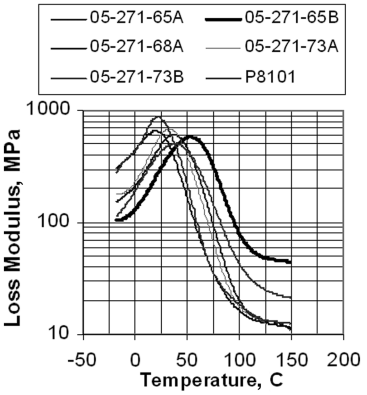

a) Epoxy-based materials @ 1 KHz

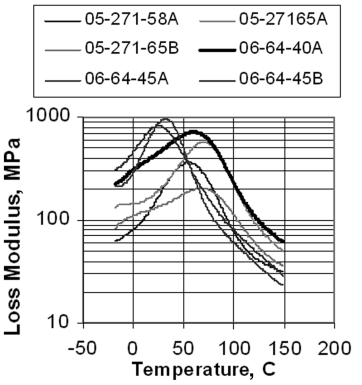

b) Waterborne materials @ 1 KHz

Fig. 6 Loss modulus of candidate materials (imaginary part of Young's modulus).

The selected materials were then modified for reduced density by the inclusion of microballoons (low-density hollow spheres) and mineral filler. The selected epoxy-based material (05-271-65B), after modification by inclusion of the microballoons and mineral filler, was designated as PPG experimental product 05-271-100C. The selected waterborne material (06-64-40A), after similar modification, was designated as PPG experimental product 05-271-99D. The epoxy-based product consisted of (essentially) 100% solids, with an estimated viscosity of 35,000–70,000 cP (35–70 Pa · s) at 40°C. The waterborne product consisted of (approximately) 75% solids with an estimated viscosity of 10,000–20,000 cP (10–20 Pa · s) at 25°C. The modified materials were then applied to test beams and the material properties determined as before. Reduced frequency nomograms for the modified materials are given in Fig. 7 and 8.

The development, description, and use of such nomograms are discussed elsewhere [4,5]. The values of the modulus are the real and imaginary parts of the Young's (tensile) modulus.

The nomograms of the two selected and modified materials were then used to estimate the total exposure time at 149°C (300°F) that would be equivalent to the entire mission profile times at temperature as given in Fig. 5. This was done by using the shift factors from a temperature of 149°C to each of the other temperature ranges to estimate, for each range of operating temperature, the equivalent time at 149°C. As a time scale is inversely proportional to a frequency scale, the shift factors for determining the equivalent times at each temperature are simply the reciprocals of the frequency shift factors already determined in the process of developing the nomograms for the materials. The sum of all of the equivalent times at 149°C was found to be slightly more than 1 h. To provide a conservative estimate of the aging effect, a 2-h exposure was used. Beam specimens coated with the two modified materials were then aged for 2 h at 149°C and retested. Nomograms of material properties were then developed again by the Öberst beam methodology. From these, the loss modulli

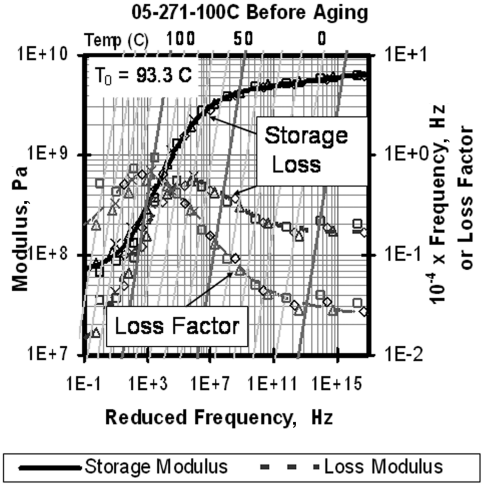

Fig. 7 Nomogram for epoxy-based fill material after modification.

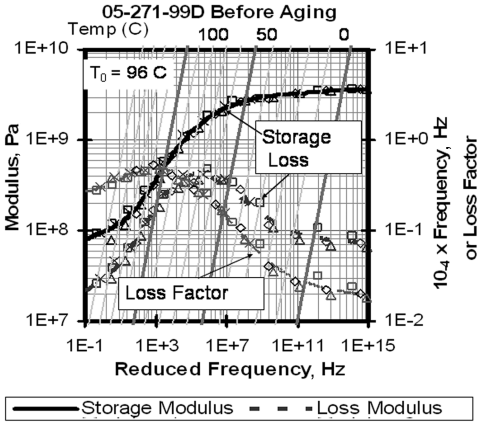

Fig. 8 Nomogram for waterborne fill material after modification.

of the modified and aged materials at 1000 Hz were found to be as shown in Fig. 9. The loss modulus is the imaginary part of the complex Young's (tensile) modulus.

For temperatures at and above room temperature, the values of the loss moduli before and after aging are seen to be essentially the same, indicating that the temperature–time history of the service life should not degrade the damping performance. A comparison of these properties with those of the unmodified materials (wide lines of Fig. 7) shows that, while inclusion of the microballoons, mineral filler, and aging reduced the loss modulus somewhat, the value remained above the desired value of 14 MPa (∼2000 psi) at all temperatures up to 149°C (300°F).

Density estimates, necessary for the determination of material properties by the Öberst method and for the prediction of the response of the filled plates, were made by taking into account both the specifications provided by PPG and the actual weights and measures of the bare strips and strips as coated with the modified materials. The estimated density of the modified epoxy-based filler is 1000 kg/m^3 (∼0.036 lb/in.^{3}); that of the modified waterborne filler is 830 kg/m^3 (∼0.03 lb/in.^{3}).

C. Assembly of Viscoelastic Material Filled Plates

Two plates were selected for testing and filled at PPG Industries, Inc. with experimental products. Plate 2 was filled with the modified epoxy-based material and plate 6 was filled with the modified waterborne product. The epoxy-based experimental product 05-271-100C was warmed up to 60°C (140°F) and poured into the plate cavity. The plate was then cured in a vertical position at 160°C (320°F) for 40 min. The water-based experimental product 05-271-99D was agitated to pourable consistency with care taken to prevent

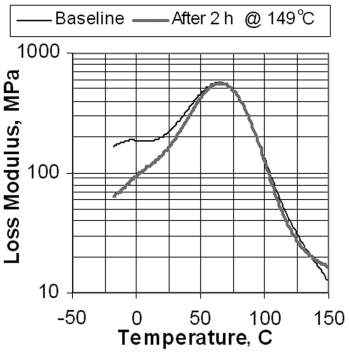

a) Epoxy-based fill (Modified) @ 1KHz

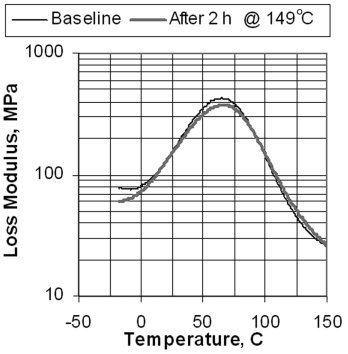

b) Waterborne fill (Modified) @ 1 KHz

Fig. 9 Young's loss modulus of modified materials, before and after aging.

air introduction. Plate 6 was filled, placed horizontally in an oven, and baked for 30 min at 82°C (180°F), followed by a 40 min bake at 140°C (284°F). Some voids are known to have been present, as may be seen in the end views and cut sections of the filled plates in Fig. 10.

The depressions seen in the end view of the epoxy filled plate (Fig. 10a) are due to a lowering of the viscosity in the curing oven, enabling material to flow away from the upper end. A small void is seen (Fig. 10d) in the waterborne filled plate in a section cut parallel to the longitudinal axis. No voids are visible in the epoxy filled plate (Fig. 10c). Sections cut parallel to the plate faces (not shown) showed no significant voids.

a) Plate 2: Epoxy fill – end view

b) Plate 6: Waterborne fill – end view

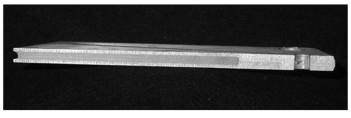

c) Plate 2: Epoxy fill – cut section

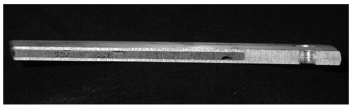

d) Plate 6: Waterborne fill – cut section

Fig. 10 Cross sections of filled specimens.

III. Test Methodology

All testing was conducted using the facilities of the Turbine Engine Fatigue Facility, Propulsion and Power Directorate, U.S. Air Force Research Laboratory, Wright–Patterson Air Force Base, Ohio. Two means of excitation were used in this study. In both cases, velocities at a station 6 mm toward the root and 6 mm toward the center from the furthest corner of the plate were measured with a laser vibrometer (Polytec® system, mode l OFV-303.8 sensor head, OFV-3001S controller, and OVD-01 velocity decoder) rated to 10 m/s. Maximum velocities in these tests were under 2.5 m/s for the unfilled plates and significantly less for the filled. The values of the system loss factor ($\eta_{sys} = 1/Q$) were found from the quality factors (Q) as determined by the vibrometer software from the bandwidth of the frequency response function. The resonant frequency was taken to be the amplitude of maximum response.

A. Excitation for Room-Temperature Determination of Amplitude Dependence

Investigations of the amplitude dependence of frequency and damping at room temperature were made with a large (Unholtz–Dickie Corporation model 560, 6000 lb force) shaker with an excitation level regulated by a PCB Piezotronics model 353 B33 quartz shear accelerometer mounted on the specimen support. The specimen was attached to the fixture by a clamping block and three bolts (see Fig. 2). System damping was determined from the bandwidth of frequency response functions obtained by holding the amplitude of the base acceleration constant and decreasing the frequency from above the resonances. Sweep rates of 8 Hz/20 min for the unfilled plates and 20 Hz/8 min for the filled plates were sufficiently low as to enable accurate capture of the frequency response function. Successive frequency response functions were obtained at increasing input accelerations. As input base accelerations did not exceed 1 g, the strain levels achieved were limited and varied between modes.

B. Excitation for Low Strain Amplitudes at Elevated Temperatures

Tests at low amplitudes of strain were conducted by exciting the specimen with a small magnet attached on the opposite side of the plate from the point at which displacements were measured. For these tests, the plates were mounted on the same shaker head, but with the shaker turned off. All modes were observed as the driving magnet was chirped from 100 to 2000 Hz over 10 s with increasing frequency. Actual values of input were not determined in these tests, but the velocity responses for these tests were found to be several orders of magnitude lower than those with the lowest practical shaker acceleration of 0.05 g.

C. Testing for Determination of Temperature Dependence

As the room-temperature response of the filled plates was found to be relatively insensitive to strain amplitude, all tests at elevated temperature were conducted with magnetic excitation and low strain amplitudes. Specimen heating was provided by the convection of hot air through a chamber with a transparent port in the top through which a laser velocimeter tracked the motion of a reflective spot attached to the specimen. After each change in temperature, a soak time of at least 60 min was allowed, with at least 30 min at constant temperature. Measurements with a thermocouple near the specimen were used to monitor and regulate the air temperature.

IV. Results of Testing at Room Temperature

A. Measurements of Natural Frequencies

The observed natural frequencies at room temperature for the first two bending modes of the plates after filling (line codes 2F and 6F) are compared with the frequencies before filling (line codes 2 and 6) in Fig. 11 . Increases in frequency resulted from the addition of both fill materials, with the shift for plate 2 (epoxy-based fill) being essentially the same as for plate 6 (waterborne fill). Although the increase is only about 3% in mode 1 (first bending), it is about 40% in the case of mode 3 (second bending) due to the increase with frequency of the storage modulus of the filler.

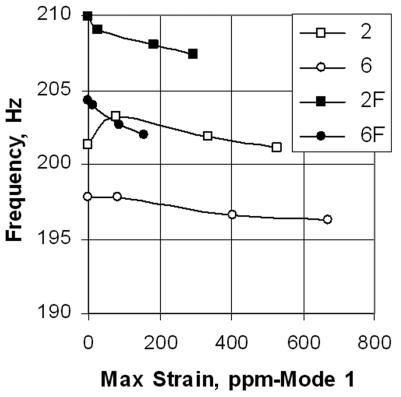

a) First bending mode

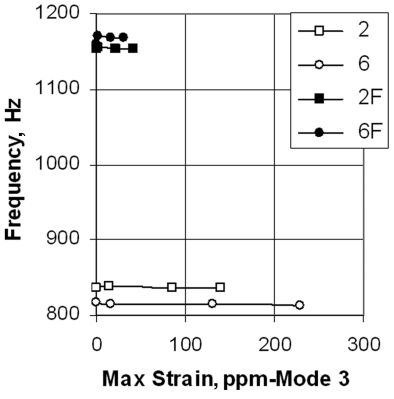

b) Second bending mode

Fig. 11 Influence of base excitation amplitude on frequencies, two modes.

The values of observed tip velocity were converted to maximum (root) strain by finite element analyses for the filled and unfilled plates. Values at the lowest level of strain were obtained with the magnetic excitation; values at the higher strains were observed with excitation by the shaker. The modest softening, evidenced by the decrease in frequency with the increase in amplitude for both the unfilled and filled plates, is likely due to support deformations or slippage in the grips rather than a softening of the filler materials.

Because the added mass serves to decrease the frequency by increasing the kinetic energy, it follows from consideration of the Rayleigh quotient that the net increase in frequency must be a consequence of a significant increase in strain energy due to addition of the filler. To the extent that additional strain energy is in the filler material, this creates the potential for high damping, especially in the third mode. Although the three higher levels of base excitation (0.05, 0.5, and 1 g) were the same in all cases, the maximum strains varied significantly between the modes. As the magnitude of the response should be proportional to the system quality factor, the large reductions in response indicate high damping in the filled blades, even at room temperature for which the fill materials were not optimized. The proportionately greater reduction in the mode 3 response indicates higher damping than in mode 1.

B. Measurements of System Damping

Initially, a series of measurements of the damping of filled plates was conducted to establish the repeatability of the measurements. The results for the first five modes are shown in Fig. 12. The numbers of tests are shown in parentheses. These tests were conducted at room temperature with a constant low level of shaker excitation (0.05 g). Variations between repeated tests for plate 6 are negligible, and only minor in the case of plate 2 for the three lower modes of interest.

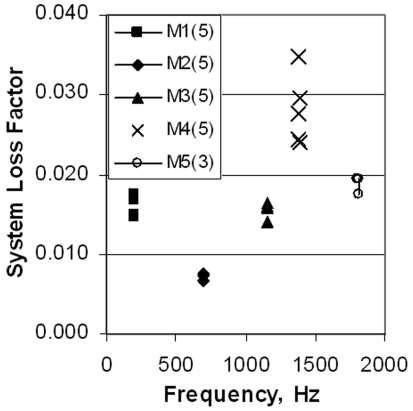

a) Plate with Epoxy-based fill

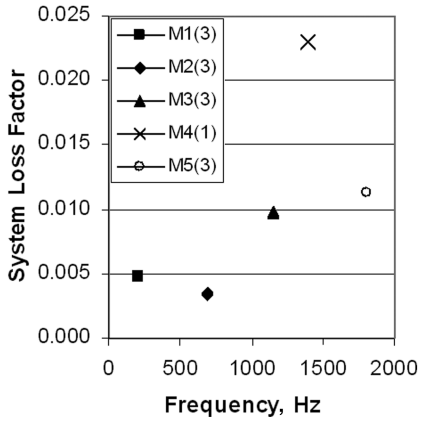

b) Plate 6 with Waterborne fill

Fig. 12 Repeatability of loss factors for filled blades (at room temperature), modes 1–5, low excitation.

The system loss factors at room temperature were also evaluated from the frequency response functions with shaker excitation levels of 0.05, 0.5, and 1 *g*. Comparisons of the system loss factors for the 1B and 2B modes with filler (line code F) and without filler (line code E) are shown in Fig. 13 for the two filler materials tested. Maximum (root) strains were estimated from the observed tip velocities by using the mode shape as determined by finite element analyses of the unfilled and filled plates. Nonlinearity of the damping is evidenced by the amplitude dependence of the loss factors for both the unfilled and filled plates. As the influence of the nonlinearity on the determination of damping from bandwidth measurements [6] should be no more than 5–7% for the filled plates and 8–12% for the unfilled, no adjustments were made. The filler is seen to add significantly to the system damping, with the epoxy-based fill providing a higher level of dissipation than the waterborne fill. Extrapolation of the limited data of Fig. 13 to low strains suggests loss factors for the bending modes are in reasonable agreement with the values at low excitation and strains shown earlier in Fig. 12.

V. Predictions and Measurements at Elevated Temperatures

A. Finite Element Modeling

The finite element analysis used to predict the natural frequencies of the filled and unfilled plates and to evaluate the stored energies in the plate and fill, respectively, were conducted using ANSYS version 10.0. The model was built using the ANSYS element SOLID92, a 10-noded tetrahedron [7]. A mesh size (LESIZE) of 6.35 mm (0.25 in.) was chosen. The model was created based on the dimensions of the hollow plate, with the small (1.6 mm or 1/16 in.) radius fillet on the inside of the hollow cavity neglected in the model. Welds were assumed to be continuous. The clamped and free ends were taken as fixed and free, respectively, in all coordinates.

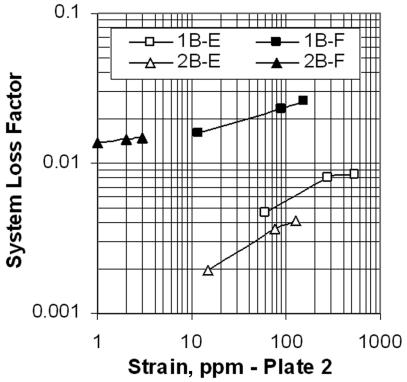

a) Epoxy-based fill

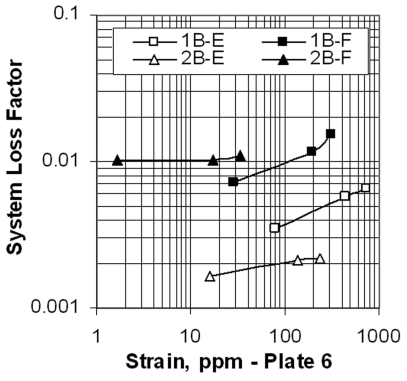

b) Waterborne fill

Fig. 13 Influence of strain amplitude on system loss factors.

Computations were made with the plate density taken as 2770 kg/m^3 (0.1 lb/in.^{3}) and a modulus of $E = 69$ GPa (107 Mpsi) at all temperatures. Nomograms for the material properties of the modified and aged materials were used to determine the storage moduli and loss factors (LF) of the fill materials at selected temperatures for frequencies representative of the three modes (M1, M2, and M3) of primary interest. The results are shown in Table 1. Values of the loss factor and storage modulus shown in italics are the values at the temperature at which the product (loss modulus) has the maximum value. The maximum value of the loss factor for each mode is in bold face. Note that the maximum value of the loss factor always occurs at a higher temperature than the maximum value of the loss modulus. Also, as the material softens with temperature, the loss modulus peak tends to move to a higher frequency (mode number).

B. Comparison of Predicted and Observed Frequencies

The predicted and observed frequencies for the unfilled and filled plates in the first three modes at temperatures up to 121°C (250°F) are shown in Fig. 14. All observed frequencies were at the low level of excitation resulting from the magnetic excitation and are notably (10 and 15%) lower than the computed values. This may be due to an inadequacy of the finite element model or an insufficient rigidity of the specimen clamping and support configuration. However, the traces in Fig. 14 of the computed and observed frequencies are essentially parallel. This indicates that the computational model is adequately representing the influence of the reduction in filler storage modulus as the temperature is increased (see Figs. 7 and 8). At the highest test temperatures, the moduli of the filler materials are essentially negligible. Consequently, the frequencies of the filled plates in the two bending modes at 121°C (250°F) are comparable to those observed (Fig. 11) for the unfilled plates at room temperature.

C. Comparison of Predicted and Observed Loss Factors

1. Methodology for Prediction of Loss Factors

The system loss factors for the filled plates were predicted from finite element analysis by using the method of modal strain energy

Table 1 Material properties at selected temperatures and frequencies

Filler Data for	Temp., °C	E-GPa (∼M1) 200 Hz	LF (∼M1) 200 Hz	E-GPa (∼M2) 700 Hz	LF (∼M2) 700 Hz	E-GPa (∼M3&4) 1200 Hz	LF (∼M3&4) 1200 Hz
Epoxy	24	4.50	0.0548	4.78	0.0471	4.78	0.0446
Epoxy	54	*2.11*	*0.264*	2.56	0.203	2.76	0.181
Epoxy	71	0.85	0.52	*1.21*	*0.431*	*1.39*	*0.393*
Epoxy	88	0.27	**0.639**	0.41	**0.634**	0.49	**0.617**
Epoxy	104	0.12	0.458	0.16	0.548	0.18	0.583
Epoxy	121	0.09	0.282	0.10	0.348	0.10	0.381
Waterborne	24	2.79	0.0669	2.92	0.0528	2.97	0.048
Waterborne	54	*1.57*	*0.268*	*1.86*	*0.213*	1.98	0.192
Waterborne	71	0.82	0.416	1.10	0.361	*1.23*	*0.335*
Waterborne	88	0.34	**0.472**	0.51	**0.464**	0.60	0.453
Waterborne	104	0.16	0.414	0.23	0.451	0.26	**0.462**
Waterborne	121	0.11	0.339	0.13	0.375	0.14	0.393

[8], modified to take into account the additional energy dissipated by the bare plate, restraining clamps, and the environment. The strain energy (U_D) in the dissipative component (filler) alone was determined by finite element analysis using the storage modulus applicable at each mode and temperature. The strain energy in the plate alone (U_P) was also found by finite element analysis and varied slightly with temperature as the mode shaped changed somewhat due to the change in the stiffness of the filler.

By definition, the system loss factor, η_{sys}, is related to the ratio of total dissipated energy to the total stored energy by

$$\eta_{\text{sys}} = \frac{D_D + D_{\text{unf}}}{2\pi U_T} \tag{1}$$

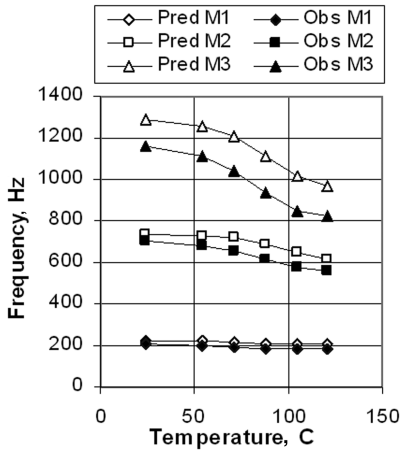

a) Plate 2 with Epoxy-based fill

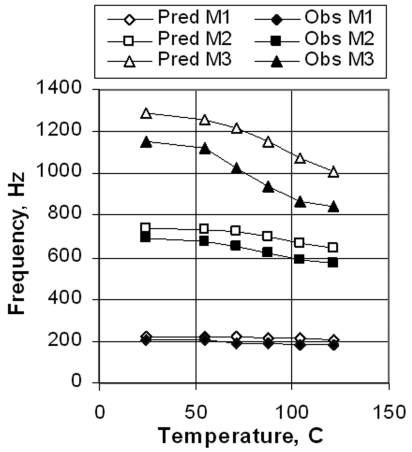

b) Plate 6 with Waterbourne fill

Fig. 14 Influence of temperature on stiffness of VEM filled plates, three modes.

where D_D is the dissipation attributed to the fill, D_{unf} is the additional dissipation due to all other sources, and U_T is the total strain energy. The definition of the loss factor

$$\eta_{\text{mat}} = \frac{D_D}{2\pi U_D} \tag{2}$$

may be used to find the energy dissipated in the filler material when the material loss factor, η_{mat}, and the strain energy in the filler material are known.

If the mode shapes for the filled and unfilled system are sufficiently similar, the additional dissipation due to the plate material, grip damping, air damping, etc., may be estimated from the measured loss factor of an unfilled plate. This additional dissipation, D_{unf}, may be evaluated by applying the definition of the loss factor to the unfilled system:

$$\eta_{\text{unf}} = \frac{D_{\text{unf}}}{2\pi U_{\text{unf}}} \approx \frac{D_{\text{unf}}}{2\pi (U_T - U_D)} \tag{3}$$

Equation (3) is only an approximation, because the strain energy in the unfilled plate, U_{unf}, will not be precisely the same as the strain energy in the plate, $U_T - U_D$, when filled, as the presence of the filler influences the mode shape.

Substitution into Eq. (1) of the dissipated energies found by solving Eqs. (2) and (3) then enables a prediction of the system loss factor from the material loss factor of the filler material, η_{mat}; the observed values of the loss factor for the unfilled plates, η_{unf}; and the ratio of the computed strain energies.

$$\eta_{\text{sys}} = \frac{\eta_{\text{mat}} 2\pi U_D + \eta_{\text{unf}} 2\pi (U_T - U_D)}{2\pi U_T} = \eta_{\text{mat}} \frac{U_D}{U_T} + \eta_{\text{unf}} \left(1 - \frac{U_D}{U_T}\right) \tag{4}$$

The contribution of the additional losses, η_{unf}, was estimated from measured loss factors for the unfilled plates at low amplitudes and room temperature. Typical values for modes 1, 2, and 3, respectively, were taken as 0.0025, 0.0019, and 0.0014 for plate 2 and 0.004, 0.0016, and 0.0013 for plate 6 (see Fig. 4b).

Equation (4) is the equation for modal strain energy [8], adjusted for losses other than those due to the filler. Note that the strain energy in the filler (U_D) must be found with the storage modulus of the filler at the frequency of the particular mode (see Figs. 7 and 8). A tendency towards overprediction of system loss factors may be expected, as the method of modal strain energy is known [9,10] to overpredict loss factors when values of the material loss factors are much greater than 0.1.

2. *Results of Comparisons*

Values obtained by applying Eq. (4) for modes 1, 2, and 3 (first bending, first torsion, and second bending) are shown in Figs. 15–17. As measured values used in these comparisons were obtained at the low strains obtained by magnetic excitation, the strains were probably 1–2 orders of magnitude less than those resulting from

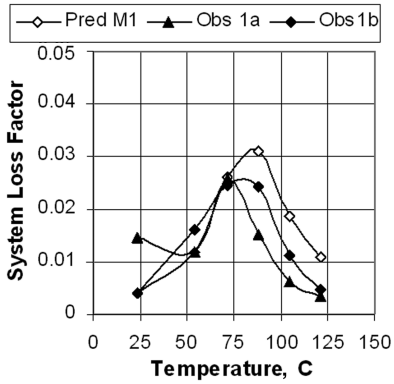

a) Plate 2 with Epoxy-based fill

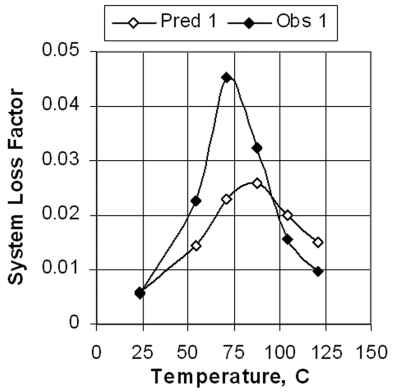

b) Plate 6 with Waterbourne fill

Fig. 15 Predicted and observed system loss factors, VEM filled, first mode.

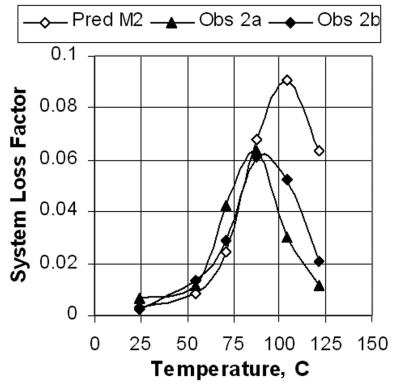

a) Plate 2 with Epoxy-based fill

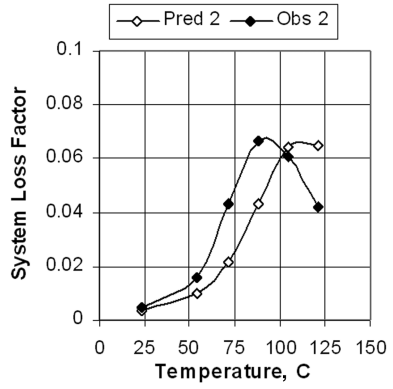

b) Plate 6 with Waterbourne fill

Fig. 16 Predicted and observed system loss factors, VEM filled, second mode.

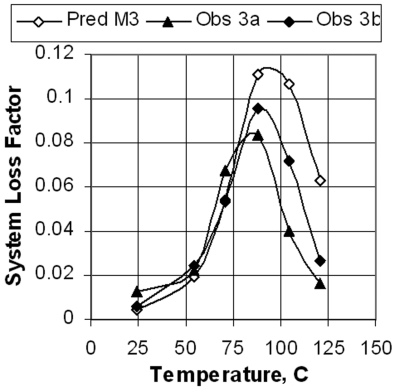

a) Plate 2 with Epoxy-based fill

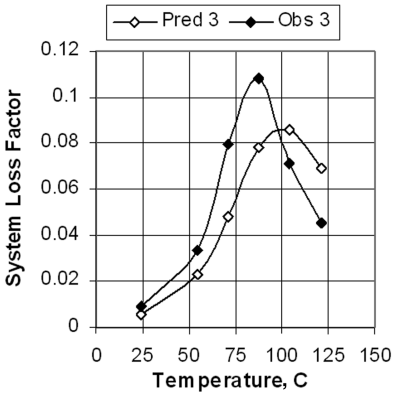

b) Plate 6 with Waterbourne fill

Fig. 17 Predicted and observed system loss factors, VEM filled, third mode.

shaker excitation at 0.05 *g*. Nonetheless, comparisons of the observations at the lowest test temperature with the room temperature measurements with a low level of shaker excitation (Fig. 12) show satisfactory agreement, as do the measurements for the bending modes at higher levels of strain, for which the loss factors (Fig. 13) are about 0.01. The repeated tests conducted on plate 2, observations (Obs) 1b, 2b, and 3b, show satisfactory agreement. The trend of increasing damping with strain amplitude provides encouragement that the damping at high strain and high temperature is likely to be even higher than the values shown in Figs. 15–17.

A comparison of predicted and observed values for the specimen with epoxy-based fill (Figs. 15a, 16a, and 17a) suggests that the predicted damping peaks are somewhat higher and occur at slightly higher temperatures than the observed. In the case of the waterborne fill (Figs. 15b, 16b, and 17b), the predicted damping peaks are somewhat lower, but again occur at slightly higher temperatures than do the observed values.

It is of interest to note the apparent superiority of the waterborne fill, especially in the first bending mode. Whereas the epoxy-based material has the higher loss modulus at 1 KHz and room temperature (Fig. 9), the loss modulus of the waterborne fill is greater for temperatures above 100°C (212°F). Consequently, although the epoxy-based material gave higher damping at room temperature (See Figs. 12 and 13), the waterborne fill gives higher damping at the higher temperatures. And, as lower frequencies are equivalent to higher temperatures (see Figs. 7 and 8), this becomes most pronounced in the case of the first mode at elevated temperatures.

3. *Discussion*

In general, the agreement between the observed and predicted loss factors is considered to be quite satisfactory in view of the fact that the storage moduli and loss factors for the filler material were obtained from tests on Öberst beams, for which the strain levels were not determined and may not have been comparable to those

encountered in the testing of the filled plates. It should also be noted that the strain distribution in the filler material when applied in a relatively thin layer on the exterior surfaces of the beams used to determine material properties may not be truly representative of the strain distribution in the filled cavities. Evidence that the strain distribution in the filled plates is not identical to the simple tension field in the strip specimens may be seen in the variation of computed values of the strain energy ratio (SER), U_D/U_T, with the storage modulus of the filler material, as shown in Fig. 18.

These computed values suggest that the strain distribution in the filler is considerably more complex than that in the case of a simple uniaxial tension. With stiff (high modulus) fillers, the face sheets of the specimen are "locked" together, and the specimen deforms essentially as a single plate. With a lower modulus, independent motion of the face sheets becomes possible, enabling additional deformations of shear and biaxial strain in the filler. By way of comparison, if a linear Bernoulli–Euler strain distribution is assumed, the strain energy ratio for a sandwich beam with a core modulus 10% of the face sheet modulus and the same thickness ratio (56%) as for the filled plates used here would be only about 2%. Values shown in Fig. 18 for the 1B and 1T modes appear to be approaching that value at a core stiffness of about 10% of plate stiffness, or around 6.9 GPa (1 Mpsi). These observations, however, do bring somewhat into question the assumption made in the development of Eq. (4) that the mode shapes of the filled and unfilled plates are the same. But in cases in which the total system loss factor is an order of magnitude greater than that of the unfilled plate, that is, $\eta_{\text{sys}}/\eta_{\text{unf}} > 10$, the resulting predictions of the system loss factor should not be sensibly influenced.

Further, it should be noted that the extraction of the storage modulus from the results of the Öberst beam tests required a priori knowledge of the density. Because the resulting values are used in the finite element analysis, all computed frequencies and strain energies, as well as predicted system loss factors, are vulnerable to error in the estimation of the filler density.

Several possible deficiencies should be noted. First, that the observed frequencies were not in as good agreement with the predicted values as might be desired. Whether this is a consequence of the inadequacy of the modeling methodology or due to inadequate specimen gripping has not been determined. Second, all testing was conducted with the blade cavity open at the free end. This is somewhat unrealistic, as the end of an actual filled blade must be closed so as to retain the filler under the high g loads resulting from blade rotation. Closing of the end can be expected to have a significant impact on the deformations in the filler material, leading to a lower strain energy density in the filler and, consequently, to lower levels of dissipation and lower values of the system loss factor.

Finally, with regard to application in an actual blade in a rotating environment, several issues not addressed here must be considered. The challenge of obtaining a complete fill in an actual blade may be significantly greater than with the specimens especially designed for ease of fill. Also, the issues of adherence of the fill material to the cavity wall and the consequences of a possible generation of a high hydrostatic pressure [11] due to centrifugal loading must be considered, although preliminary studies [12] have suggested that this may not be a problem. And finally, in an actual blade, the variations of temperature throughout the blade and filler material must be taken into account.

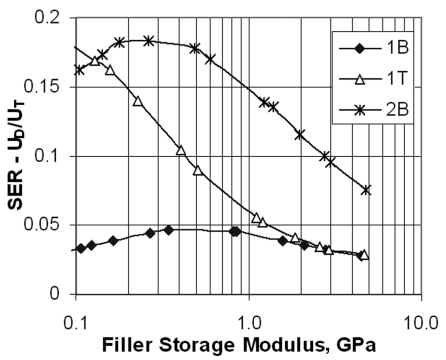

Fig. 18 Filler strain energy (SER) as fraction of total.

VI. Conclusions

A hollow plate of trapezoidal planform was designed, fabricated, and tested without filler and with two different fillers selected as having significant potential as fill materials for a hollow fan blade as used in a gas turbine engine. The specimen planform was designed to be roughly representative of such blade geometries, but of sufficient simplicity to ensure achieving nearly 100% fill while enabling a relatively modest finite element model to adequately represent the configuration.

The observed values of loss factors in the filled plates are much greater than can be accounted for by assuming that the strain distribution in the filler is simply that arising from a linear thicknesswise variation in uniaxial bending strain with negligible shear deformation. It is suggested that the relatively thin cavity skins undergo additional deflections, especially localized longitudinal and chordwise bending, and that in these deformations the plates are not well coupled, enabling the development of significant additional deformations in the filler.

All three of the primary objectives of the effort were achieved. First, it was demonstrated that filling the cavity of a hollow bladelike plate with a relatively lightweight viscoelastic filler material could produce significant increases in the system damping. The filler materials used increased the weight per unit area over the portion of the blade with cavity by less than 50%, while reducing the system quality factor (Q) by about 1 order of magnitude in the first bending mode and significantly more in the second bending mode. The hollow plate developed for this study appears to be suitable for further use in comparing the effectiveness of candidate filler materials.

Second, filler materials were identified that were capable of producing high levels of system damping at elevated temperatures after being subjected to an aging treatment conservatively estimated to be equivalent to 4000 h of service at a characteristic mission profile. Two classes of fill material were considered: epoxy based and waterborne. In each case, a material was found that demonstrated a high loss modulus over the temperature range of interest, even after reducing the effective density by the inclusion of hollow spheres and mineral filler and applying the aging process. The filled plates were found to have values of system Q for bending modes ranging from 5 to 20 times less than those of the unfilled plates at temperatures of 65–95°C (150–200°F).

And finally, the generally good agreement found between the predicted and observed system loss factors suggests that predictive tools such as those employed here should enable successful predictions of the increased damping that can be obtained by filling actual blades with similar materials, in spite of differences in blade materials, the more complex geometries, and nonuniform temperature distributions and core thicknesses.

The maximum loss factors observed for the bladelike structures considered in this study correspond to system quality factors ($Q = 1/\eta$) in the ranges of 22–40, 16–17, and 9–11 for the first three modes, respectively. Rongong and Williams have reported [3] the prediction and observation of maximum quality factors in the range of 25–50 for a large civil fan blade filled with an epoxy-based compound and glass and polymeric microballoons. Taken together, these results suggest that filling the cavities of hollow blades with a low density viscoelastic fill offers promise of significant increases in blade damping and the concomitant reduction of resonant response.

Acknowledgments

The authors are indebted to the Propulsion and Power Directorate of the U.S. Air Force Research Laboratory, Wright–Patterson Air Force Base, Ohio, for making the facilities of the Turbine Engine Fatigue Facility available for this study. Financial support was

provided to Universal Technology Corporation by the United States Air Force under contract no. F33615-02-D-2299.

References

[1] Norris, J. M., Knott, D. S., Jones, A. M., Mideglow, D. R., and Hall, R. M., Turbomachine Blade, US Patent No. 6,669,447, 30 Dec. 2003.

[2] Gordon, R. W., and Hollkamp, J. J., "An Internal Damping Treatment for Gas Turbine Blades," AIAA Paper 1997-1154, April 1997.

[3] Rongong, J. A., and Williams, R. J., "Lightweight, Polymeric Cavity Filler for Damping Hollow Fan Blade Vibrations," *Proceedings of the 9th National Turbine Engine High Cycle Fatigue (HCF) Conference* [CD-ROM], Session 12b, No. 1, Universal Technology Corporation, Dayton, OH, 2004.

[4] Nashif, A. D., Jones, D. I. G., and Henderson, J. P., *Vibration Damping*, Wiley, New York, 1985.

[5] Jones, D. I. G., *Viscoelastic Vibration Damping*, Wiley, New York, 2001.

[6] Torvik, P. J., "A Note on the Estimation of Non-Linear System Damping," *Journal of Applied Mechanics*, Vol. 70, May 2003, pp. 449–450.
doi:10.1115/1.1571859

[7] ANSYS Documentation for Release 10.0, SAS IP, ANSYS, Inc., Canonsburg, PA, 2005.

[8] Johnson, C. D., and Kienholz, D. A., "Finite Element Prediction of Damping in Structures with Constrained Viscoelastic Layers," *AIAA Journal*, Vol. 20, No. 9, Sept. 1982, pp. 1284–1290.

[9] Torvik, P. J., and Runyon, B. D., "Observations on the Accuracy of Finite Element Predictions of Constrained Layer Damping," *Proceedings of the 10th National Turbine Engine High Cycle Fatigue (HCF) Conference* [CD-ROM], Session 1B, No. 3, Universal Technology Corporation, Dayton, OH, 2005.

[10] Torvik, P. J., and Runyon, B. D., "Modifications to the Method of Modal Strain Energy for Improved Estimates of Loss Factors for Damped Beams," *Shock and Vibration*, Vol. 14, No. 5, Sept. 2007, pp. 339–353.

[11] Gordon, R. W., and Hollkamp, J. J., "A Comparison of Damping Treatments for Gas Turbine Engines," *Proceedings SPIE Smart Structures and Materials, 1996: Passive Damping and Isolation*, edited by C. D. Johnson, Vol. 2720, Society of Photo-Optical Instrumentation Engineers, Bellingham WA, 1996, pp. 2–12.

[12] Flint, E. M., Rogers, L., and Fowler, B. L., "Viscoelastic Material Properties in a High Pressure Environment," *Proceedings of the 3rd National Turbine Engine High Cycle Fatigue Conference* [CD-ROM], Session 11, No. 1, Universal Technology Corporation, Dayton, OH, 1998.

A. Prasad
Associate Editor